ELSEVIER

Chemical Engineering Journal 72 (1999) 63–77

Chemical Engineering Journal

Individual and simultaneous desorption of H_2S and CO_2 from synthetic green liquor

Andreas Hinz*, Mats Wallin

Department of Chemical Engineering II, Center for Chemistry and Chemical Engineering, Lund University, P.O. Box 124, SE-22100, Lund, Sweden

Received 11 September 1998; received in revised form 27 October 1998; accepted 3 November 1998

Abstract

Selective desorption of H_2S from green liquor has been investigated using a batch stirred tank reactor. It was found that the gas and liquid side resistances are dependent on the stirrer velocity. In this equipment for physical absorption and desorption of H_2S or CO_2 the resistance in the liquid side is dominant. Within the pH interval researched, the individual desorption rate of CO_2 as well as H_2S is mainly determined by the liquid side mass transfer rate and is not enhanced by any reaction in the film. For the desorption of H_2S from a Na_2S solution, an equilibrium model based on the film theory was evaluated. Another model also based on the film theory with finite reaction rate in the film as well as in the bulk was evaluated for the desorption of CO_2 from $NaHCO_3$ solution. Both models show values which are in good agreement with the experimental results. For the desorption of H_2S from synthetic green liquor a model was taken from the literature [M. Wallin, S. Olausson, Chem. Eng. Commun. 123 (1993) 43–59] and modified. The modified model takes into account that the desorption of H_2S from synthetic green liquor is enhanced by the chemical reaction from hydrogencarbonate to carbonate. The desorption of CO_2 from synthetic green liquor is well described by the model evaluated for the individual desorption of CO_2 from $NaHCO_3$ solution.

Keywords: Desorption; Film theory; Synthetic green liquor

1. Introduction

The latest evolution step of technology for handling black liquor in the pulp and paper industry is the installation of a pressurised gasification plant [1]. The installation of a pressurised black liquor gasification plant is also a method of debottlenecking a mill with limited chemical recovery capacity. Chemicals of interest for recovery are sulphur and sodium in their different forms. Using modern gas cleaning technology, the outcoming stream from the gasification plant can be split into separate streams and the emissions from the process can be kept very low.

After gasification of black liquor, sulphur is primarily found as H_2S in the product gas and Na_2S/NaHS in the inorganic liquid phase. The distribution of these two compounds depends on the gasification conditions. CO_2 has been produced during the gasification process and is also present in the outcoming gas stream. With acid gas absorption and subsequent stripping, the outcoming gas stream can be cleaned. This means that H_2S is absorbed into a solution (can be one of the alkaline liquor streams) and the remaining gas has turbine fuel quality. After the absorption step, the H_2S rich solution is sent into a stripper and the H_2S is desorbed, yielding two process streams. One stream contains H_2S and the other contains sulphur-free alkali carbonate. This is the point where the process opens up many new possibilities of using the mass streams.

For example, the stream of concentrated H_2S can be used for:

1. Absorption into green or white liquor.
2. Oxidation into elementary sulphur.
3. Oxidation into SO_2.

The sulphur-free alkali stream can be used:

1. In the oxygen delignification and bleaching process
2. As a part of the sulphite cooking liquor.

This is the theory but not the reality, as there is the problem of the simultaneous desorption (absorption) of carbon dioxide and hydrogen sulphide. The selectivity for

*Corresponding author. Fax: +46-46-149156; e-mail: andreas.hinz@chemeng.lth.se

1385-8947/99/$ – see front matter
PII: S1385-8947(98)00146-6

H_2S over CO_2 is not high enough to achieve a satisfactory hydrogen sulphide removal efficiency. CO_2 will also be removed in rather large quantities, making the process uneconomic and shift it far away from the ideal case [2]. Describing the co-desorption of hydrogen sulphide and carbon dioxide from green liquor requires knowledge about the affecting factors. With knowledge about these factors it is possible to optimise the existing process or to find new solutions.

Previous research in this area is very rare and most publications deal with selective absorption of H_2S and/or CO_2 from gas phases into liquid phases. Anyway, according to the literature [3,4] the problem of desorption is related to absorption and a review of earlier publications, dealing with absorption, is given here.

Yih and Sun [5] studied the simultaneous absorption of H_2S and CO_2 into potassium carbonate solution with or without amine promoters. They report that the CO_2 absorption rate increases rapidly with increasing liquid flow rate and only slightly with increasing gas flow rate. For the absorption of CO_2 they further claimed that it is a liquid film mass transfer controlled process. The absorption rate of H_2S increases rapidly with increasing gas flow rate and only slightly with increasing liquid flow rate in their experiments. They concluded that the absorption reaction of H_2S into K_2CO_3 solution can be regarded as a gas film controlled process.

Yih and Lai [6] studied the simultaneous absorption of CO_2 and H_2S in hot carbonate solutions in a packed absorber–stripper unit. They report that the performances of the absorber and stripper are strongly coupled with each other. They found that in the absorber the CO_2 is liquid phase mass transfer controlled and H_2S is gas phase controlled. In the stripper, H_2S is gas phase controlled and CO_2 is both gas and liquid phase controlled.

Wallin and Olausson [7] studied the absorption of H_2S and CO_2 into a solution of sodium carbonate using an absorption tower filled with Raschig rings. They claim that the pH value must be in the range of 9–12 as at higher pH values the absorption of CO_2 is turned into the gas side mass transfer dominant region. At pH values lower than 9 they claim that the strong enhancement effect from the dissociation reaction of H_2S will be lost. The selectivity for H_2S absorption increased with an increasing gas flow rate in their experiments.

McKeough [2] studied the recovery of H_2S formed during black liquor gasification. H_2S has been directly absorbed into green liquor in this study and it was found that direct absorption of H_2S into green liquor seems to be feasible if the mass transfer resistance in the gas phase is low.

2. Experimental setup

The test facility consists of three main parts, namely the stirred tank reactor, a mass spectrometer and a pH-stat, see Fig. 1. A benefit with the stirred tank reactor is that the interfacial area of desorption (absorption) process is exactly known. To obtain an almost perfectly mixed liquid phase, the reactor is equipped with a liquid impeller and baffles-plates. The mixing of the gas phase is supported by a gas impeller. From the design point of the reactor, the installation dimensions of the impellers are of importance. The impellers affect the desorption behaviour of the system to a larger extent due to their influence of the mixing behaviour of both phases in the reactor. Figs. 2 and 3 show both impellers with their installation dimensions in the reactor.

The temperature and the pH value of the liquid phase as well as the flow rate and pressure of the gas flow are measured and regulated. Furthermore the stirrer velocity is measured. In the literature [3,8–11] it is mentioned that the desorption rate (absorption rate), among other things, is a function of the stirrer velocity (Reynolds number). Therefore, a stirrer motor with high accuracy is used. The desorption rate also depends upon specific aspects, like design and location of the baffles, shape and location of the impeller, diameter and height of the vessel and location of gas in and outlets [12–17]. These technical data of the stirred tank reactor are shown in Table 1.

To scan the processes occurring during the experiments, a pH-stat is used as an indicator and a mass spectrometer as an analytical support. The pH-stat is connected with a computer to register the amount of buffer solution added to the solution in the stirred tank reactor, as a function of time. The amount of added buffer solution corresponds to the amount of desorbed H_2S and CO_2 from a Na_2S or $NaHCO_3$ solution, respectively. In the experiments for detection of the gas and liquid side mass transfer resistances, the pH-stat shows the amount of absorbed SO_2 and CO_2. Special attention was paid to the volume of added buffer solution due to the batch wise run mode of the stirred tank reactor. As a maximum value of added buffer solution in one experiment, a value of 2–5% of the start liquid volume was chosen. This amount of added volume should then be low enough not to disturb the experimental conditions.

For the detection of the amounts of H_2S and CO_2 simultaneously desorbed from green liquor a mass spectrometer was used. During these experiments the pH value and the purge gas flow were also held constant. Measuring the amount of H_2S and CO_2 with a mass spectrometer is a common method in such experiments [7,18]. A simple

Table 1
Technical data of the stirred tank reactor

Gas volume	3 dm^3
Liquid volume	5 dm^3
Interfacial area	241 cm^2
Stirrer velocity	50–350 rpm
Pressure	1 atm
Temperature	20–45°C
Fluid impeller diameter	10.1 cm
Gas impeller diameter	11.8 cm
Reactor diameter (inside)	17.8 cm

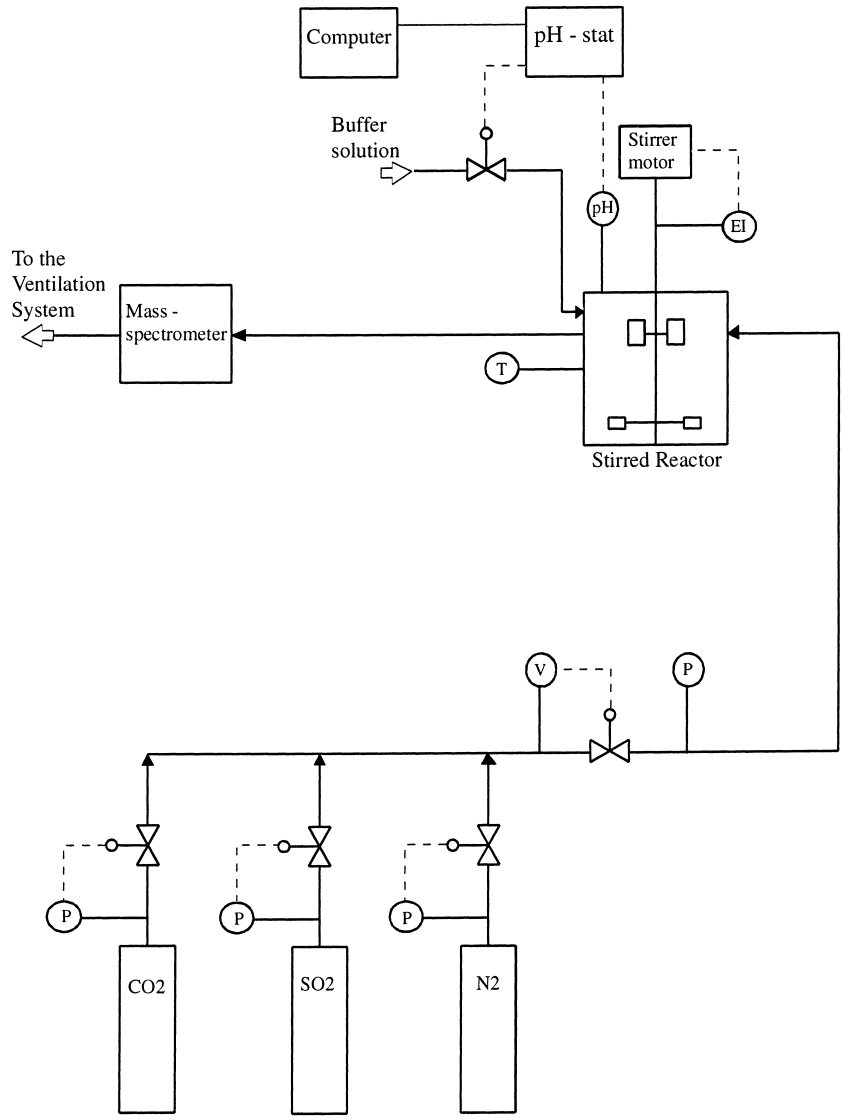

Fig. 1. The test facility used for the experiments.

analysis matrix with only H_2S, CO_2 and Ar as standard substances has been used. To measure in the ppm range, especially in the lower ppm range, a background measurement was performed for each calibration and experiment with the mass spectrometer. The relatively high background might falsify the results if not subtracted [19].

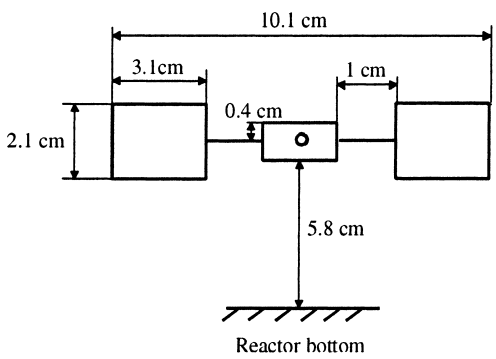

Fig. 2. The liquid impeller, equipped with four stirrer blades.

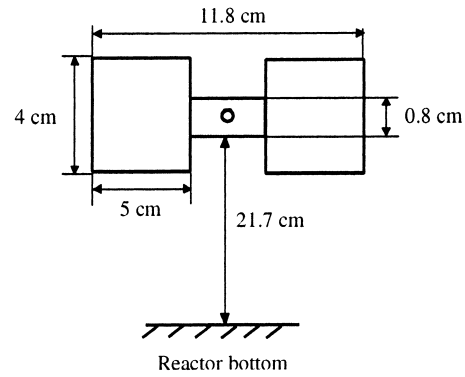

Fig. 3. The gas impeller, equipped with two stirrer blades.

As mentioned above the purge gas flow was held constant due to its impact on the gas side mass transfer coefficient. However, the gas side mass transfer coefficient is mainly determined by the gas stirrer rate. Nitrogen was chosen to be the purge gas as it is inert with respect to oxidation/reduction reactions of the desorbing compounds.

3. Calibration of the reactor

3.1. Determination of the liquid side mass transfer coefficient

The liquid side mass transfer coefficient is easily determined in a system where the gas side resistance is negligible. Such a reaction is the absorption of pure CO_2 in an aqueous alkaline solution [3]. Following mechanisms may occur:

$$\text{at pH} > 8 \quad CO_2 + OH^- \rightarrow HCO_3^- \tag{1}$$

$$\text{at pH} < 8 \quad CO_2 + H_2O \rightarrow HCO_3^- + H^+ \tag{2}$$

Depending on the adjusted pH value the reverse reaction between HCO_3^- and CO_3^{2-} has also to be considered:

$$HCO_3^- + OH^- \leftrightarrow CO_3^{2-} + H_2O \tag{3}$$

The liquid side mass transfer coefficient k_L was detected by absorption experiments of pure CO_2 into an aqueous NaOH solution. These experiments were performed at different pH values (8, 11 and 12), temperatures (20°C and 45°C) and stirrer velocities (50–350 rpm). For calculation of the k_L value the equation for physical absorption has been used:

$$Ra = k_L a(A' - A^0) \tag{4}$$

where R is the absorption rate (kmol m^{-2} s^{-1}); a represents interfacial area (m^2), k_L is the liquid side mass transfer coefficient (m s^{-1}), A' represents the concentration of dissolved CO_2 gas at the interface, in equilibrium with gas atmosphere (kmol m^{-3}), A^0 is the concentration of CO_2 in the liquid bulk (kmol m^{-3}).

The value of A' is calculated according to Henry's law, given by the following equation:

$$A' = \frac{P_A}{He_A} \tag{5}$$

where P_A is the partial pressure of CO_2 (105 Pa), He_A represents Henry's law constant (Pa m^3 kmol^{-1}).

To prove that Eq. (4) is applicable without enhancement factor, a set of calculations has been performed. Following equations [3] are applicable for the calculation of the enhancement factor of a second-order reaction:

$$E = \frac{\sqrt{(M(E_i - E)/(E_i - 1))}}{\tan h\sqrt{(M(E_i - E)/(E_i - 1))}} \tag{6}$$

Table 2
Numerical values of the constants used in the calculations

	20°C	45°C
k_{OH} (m^3 kmol^{-1} s^{-1})	5700	33980
D_A (m^2 s^{-1})	1.77×10^{-9}	3.16×10^{-9}
D_B (m^2 s^{-1})	4.66×10^{-9}	8.32×10^{-9}
He_A (Pa m^3 kmol^{-1})	25700	47200

$$M = \frac{D_A k_{OH} B^0}{k_L^2} \tag{7}$$

$$E_i = 1 + \frac{D_B B^0}{b D_A A'} \tag{8}$$

where E is the enhancement factor, E_i represents enhancement factor for an instantaneous reaction, D_A is the diffusivity of dissolved CO_2 (m^2 s^{-1}), k_{OH} represents reaction rate constant for Eq. (1) (m^3 kmol^{-1} s^{-1}), B^0 represents concentration of OH^- ions in the liquid bulk (kmol m^{-3}), b is the stoichiometric factor, $b = 2$ at pH 11 and 12, and $b = 1$ at pH 8, D_B is the diffusivity of OH^- ions in the liquid bulk (m^2 s^{-1}).

The values for k_{OH}, He_A, D_A and D_B are calculated from equations given in the literature [7]. The values for all constants in the given equations are listed in Table 2.

At the pH values used, Eq. (8) shows E_i values close to 1. Performing the iterative calculation of E with Eq. (6), a value of approximately 1 is found. The physical meaning behind these calculations and obtained results is that no enhancement effect from the chemical reaction occurs in the film between liquid bulk phase and gas bulk phase. This is due to the large amount of CO_2 pressed into the film. Even if the absorption of CO_2 is fast or instantaneous, large amount of CO_2 shifts the reaction plane from the interface between gas and liquid films to the interface between liquid film and liquid bulk phase.

For the obtained values of k_L see Fig. 4, the k_L values are shown as a function of stirrer velocities. The log–log plot generates a linear dependency. The function describing the dependency is:

$$k_L = d\left(\frac{U}{60}\right)^m \tag{9}$$

where k_L is the liquid side mass transfer coefficient based on CO_2 absorption (m s^{-1}), d is the pre factor, m represents the exponent, U is the stirrer velocity (rpm).

From Fig. 4 the following values are obtained using a least squares fit: $d = 2.90 \times 10^{-5}$ (m s^{-1}), $m = 1.60$.

3.2. Determination of the gas side mass transfer coefficient

The gas side mass transfer coefficient k_G is determined by the absorption of a gas followed by an instantaneous irre-

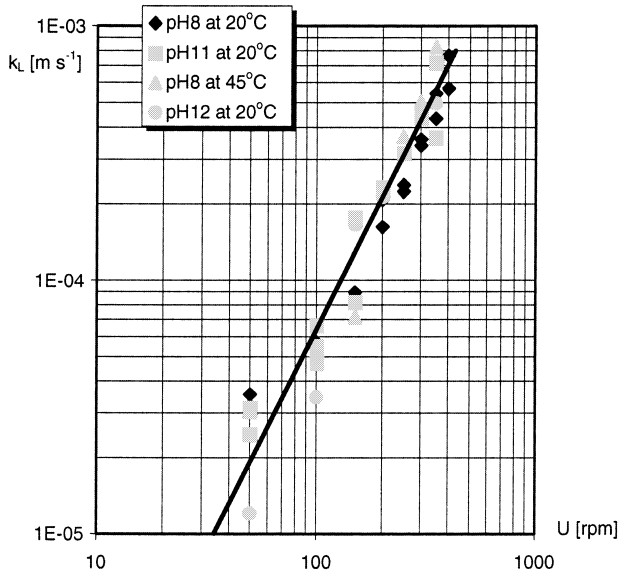

Fig. 4. k_L value vs. stirrer velocity.

versible reaction. Such a reaction is, for example, the absorption of SO_2 into a NaOH solution. The following reaction occurs:

$$SO_2 + OH^- \rightarrow SO_3^{2-} + H_2O \quad (10)$$

In the present case a gas mixture containing 1000 ppm SO_2 and 99.9% N_2 was used. It was assumed that the composition of the atmosphere over the liquid phase is constant, even if small amounts of SO_2 were absorbed into the liquid phase. This assumption of steady state with respect to the gas atmosphere is possible due to the high gas flow through the reactor and introduces a maximum error of 20%.

Depending on the concentrations of the reactants the concentration profiles for the instantaneous reaction vary [3]. The basic equation for determining k_G is:

$$Ra = k_G a(A - A')\mathrm{He} \quad (11)$$

where R is the absorption rate (kmol m^{-2} s^{-1}), a represents interfacial area (m^2), k_G is the gas side mass transfer coefficient (kmol Pa^{-1} m^{-2} s^{-1}), A is the concentration of SO_2 in the gas phase (kmol m^{-3}), A' represents concentration of dissolved SO_2 gas at the interface, in equilibrium with gas at the interface (kmol m^{-3}), He denotes Henry coefficient of SO_2 (Pa m^3 kmol^{-1}).

If the reaction plane is identical to the gas–liquid interface, the k_G values are easily evaluated by adjusting $A' = 0$. If the concentration of the absorbing gas is too high, then the interface between liquid side and gas side is not identical with the reaction plane. In this case the reaction plane is located in the film between the gas–liquid interface and liquid bulk phase. Eq. (12) is employed to calculate the real k_G value in such a situation [3], and the values of the constants used are given in Table 3:

Table 3
Numerical values of the constants used in the calculations

	20°C	45°C
D_A (m^2 s^{-1})	1.77×10^{-9}	3.16×10^{-9}
D_B (m^2 s^{-1})	4.66×10^{-9}	8.32×10^{-9}
He_A (Pa m^3 kmol^{-1})	58 000	15529

$$k_G = \frac{1}{\left[1/R((D_B B^0/D_A b) + (P_A/He_A)) - 1/k_{AL}^0\right]He_A} \quad (12)$$

where R is the experimentally detected absorption rate (kmol s^{-1} m^{-2}, D_B is the diffusivity of OH^- ion in the liquid phase (m s^{-1}), B^0 represents OH^- concentration in the liquid bulk phase (kmol m^{-3}), D_A is the diffusivity of SO_2 in the liquid phase (m s^{-1}), b is the stoichiometrical factor = 1, P_A represents partial pressure of SO_2 in the gas phase (Pa), He_A denotes Henry coefficient of SO_2 (Pa m^3 kmol^{-1}), k_{AL}^0 represents mass transfer coefficient of SO_2 in the liquid phase without chemical reaction (m s^{-1}).

The experiments for determination of the k_L values at pH 8 are used to calculate the values of k_{AL}^0. This is possible by the following correlation:

$$k_{AL}^0 = k_{BL}^0 \frac{D_A}{D_B} \quad (13)$$

where k_{BL}^0 represents experimentally detected k_L values for CO_2 at pH 8 (m s^{-1}), D_A is the diffusivity of SO_2 (m^2 s^{-1}), D_B represents the diffusivity of CO_2 (m^2 s^{-1}). Fig. 5 show the experimentally obtained k_G values versus the stirrer velocities. Analogously with Eq. (9) the log–log plot shows

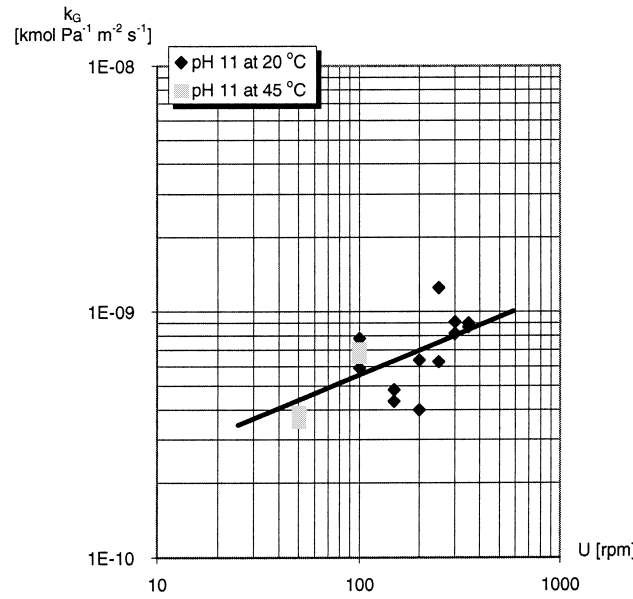

Fig. 5. k_G value vs. stirrer velocity.

an approximately linear dependency:

$$k_G = d\left(\frac{U}{60}\right)^m \quad (14)$$

where k_G is the gas side mass transfer coefficient based on SO_2 absorption (kmol Pa^{-1} m^{-2} s^{-1}), d is the pre factor, m is the exponent, U is the stirrer velocity (rpm).

From Fig. 5 the following values are obtained: $d = 4.0 \times 10^{-10}$, $m = 0.37$.

Correlation in the form of Eqs. (9) and (14) or in similar form are often used to describe the dependency of k_L and k_G by different variables [10,12–17,20,21]. Focusing more on the literature [12–15,17,21] one will find that the values which describe the effect by the stirrer velocity are largely scattered. Values are given for m which are in the range between $m = 0.7$ and $m = 3$. This depends on the different system properties, and it is claimed that no universal applicable correlation is yet available [12–14]. Another aspect is the limited availability of correlated values for k_G [16] as the volumetric liquid side mass transfer coefficient is the predominant parameter in reactor design for agitated gas–liquid contactors [20]. All these facts make it very difficult to compare the obtained m-values from the present study with the values given in the literature. The only conclusion that can be made is that our m-values are in the range which is given in the literature.

4. Individual desorption of H_2S and CO_2

H_2S has been desorbed from a Na_2S solution of concentration 0.075 kmol m^{-3}. CO_2 has been desorbed from a $NaHCO_3$ solution with concentration 0.2 kmol m^{-3}. These experiments were performed at different stirrer velocities, 50–300 rpm, and at different pH values, pH 9 and 10. The obtained desorption rates versus stirrer velocities are shown in Tables 4 and 5.

H_2S and CO_2 were first desorbed individually as there might be an interaction between them when they desorb, analogous to the absorption process [22]. These experiments were performed to observe this difference and to see how far a model is applicable, developed under the assumption that either gas is inert in the desorption process. Different stirrer velocities were chosen due to the effect on the mass transfer coefficients. They are affected as the Reynolds number has an effect on the liquid film thickness at the interface [5]. The pH values are chosen to be pH 10 and 9 as the driving force for desorption must be sufficiently high and the composition not too far away from an ordinary green liquor. The purge gas flow was adjusted to be large enough to remove the desorbed gases immediately from the reactor and prevent a build up of H_2S or CO_2 in the gas phase slowing down the desorption process. This gives the requirement for the assumption that the concentration of H_2S and CO_2 is equal to zero in the gas bulk. A maximum error of about 10–20% might be introduced for H_2S desorption and about 10% for CO_2 desorption by this assumption. The error estimations were calculated assuming a well mixed gas phase above the liquor surface with a CO_2/H_2S gas input from desorption and a CO_2/H_2S gas output via exiting purge gas (CSTR reactor approach). Inflow purge gas contains no CO_2/H_2S gas output via exiting purge gas (CSTR reactor approach). Inflow purge gas contains no CO_2/H_2S species. Build-up concentrations may be calculated via a material balance of CO_2 and H_2S, respectively. The maximum desorption rates were used and the maximum error was calculated as the ratio between gas phase build-up and driving force for desorption in liquid of each component (in corresponding units).

Table 4
Desorption rates of CO_2 at pH 9 and 10

U (rpm)	R (kmol m^{-2} s^{-1}) pH 9	R (kmol^{-2} s^{-1}) pH 10
50	8.21×10^{-9}	1.85×10^{-9}
50	3.43×10^{-9}	1.93×10^{-9}
100	1.58×10^{-8}	2.43×10^{-9}
100	1.91×10^{-8}	1.72×10^{-9}
150	1.67×10^{-8}	4.32×10^{-9}
150	2.38×10^{-8}	4.06×10^{-9}
200	6.29×10^{-8}	9.59×10^{-9}
200	8.36×10^{-8}	1.16×10^{-8}
250	9.78×10^{-8}	7.21×10^{-9}
250	9.52×10^{-8}	1.02×10^{-8}
300	1.32×10^{-7}	1.96×10^{-8}
300	1.36×10^{-7}	1.58×10^{-8}

Table 5
Desorption rates of H_2S at pH 9 and 10

U (rpm)	R (kmol m^{-2} s^{-1}) pH 9	R (kmol m^{-2} s^{-1}) pH 10
50	8.14×10^{-9}	6.72×10^{-9}
50	1.06×10^{-8}	5.16×10^{-9}
100	1.66×10^{-8}	5.40×10^{-9}
100	1.78×10^{-8}	9.01×10^{-9}
150	1.03×10^{-8}	9.25×10^{-9}
150	2.22×10^{-8}	4.70×10^{-9}
200	4.42×10^{-8}	6.53×10^{-9}
200	5.15×10^{-8}	1.29×10^{-8}
250	8.23×10^{-8}	1.68×10^{-8}
250	7.97×10^{-8}	1.05×10^{-8}
300	1.11×10^{-7}	1.55×10^{-8}
300	1.12×10^{-7}	2.71×10^{-8}

5. Modelling the individual desorption of H_2S and CO_2

5.1. Desorption model for H_2S

At pH 9 and 10, the desorption process of H_2S can be described by the equation:

$$HS^- + H^+ \leftrightarrow H_2S\,(aq) \quad (15)$$

5.1.1. Model A

The reaction from Eq. (15) is instantaneous and at equilibrium it can be expressed by the following equation:

$$K_1 = \frac{a_{HS^-} a_{H^+}}{a_{H_2S}} \tag{16}$$

where K_1 is the equilibrium constant (kmol m^{-3}), a_i denotes the activity of species i.

At steady state the H_2S (aq) formed in Eq. (15) is totally desorbed from the liquid phase and the enhancement factor is equal to 1:

$$R = K_L\left([H_2S] - [H_2S]^0\right) \tag{17}$$

where R is the desorption rate (kmol m^{-2} s^{-1}), K_L denotes the overall mass transfer coefficient for H_2S based on the liquid side (m s^{-1}), $[H_2S]$ represents concentration of H_2S in the liquid bulk phase (kmol m^{-3}), $[H_2S]^0$ is the concentration of H_2S in the liquid bulk phase (kmol m^{-3}).

Further it is assumed that the concentration of H_2S in the gas phase $[H_2S]^0$ is zero due to the small amount of desorbed H_2S and the continuous purge flow of nitrogen. This modifies Eq. (17) into the form:

$$R = K_L[H_2S] \tag{18}$$

The overall mass transfer is calculated from the following equation:

$$K_L = \frac{1}{k_G He} + \frac{1}{k_L E} \tag{19}$$

where k_G is the gas side mass transfer coefficient (kmol Pa^{-1} m^{-2} s^{-1}), He represents Henry coefficient (Pa m^3 kmol^{-1}), k_L is the liquid side mass transfer coefficient (m s^{-1}), E is the enhancement factor (in Model A, $E = 1$).

The gas and liquid side mass transfer coefficients for H_2S are evaluated from the experimentally detected values given in Section 3. For converting the values from one species to another, Eq. (13) is valid.

The rearranged Eq. (16) combined with Eq. (18) gives the final expression for the desorption of H_2S:

$$R = K_L \frac{[HS^-][H^+]}{K_1} \tag{20}$$

5.1.2. Model B

Another model was taken from the literature [7] and considers the enhancement of the desorption process by chemical reaction. The model is based on the film theory and considers the transport process for the species H_2S (aq), HS^-, H^+ and OH^-. The species S^{2-} is not included since the second dissociation of H_2S can be neglected due to its high pK_a value, $pK_a \approx pK_w + 1.74 \approx 15.74$. From the film model, neglecting the potential gradients induced by ionic flux:

$$\frac{d}{dx}\left(D_i \frac{dC_i}{dx}\right) + r_i = 0 \tag{21}$$

where D_i is the diffusivity of the species (m^2 s^{-1}), c_i represents the concentration of the species (kmol m^{-3}), x is the distance (m), r_i is the rate of reaction (kmol m^{-3} s^{-1}).

In a real system, the potential gradients will be dispersed by large amount of inert ionic species present. The flux rate of the species i at any position is given by:

$$N_i = -D_i \frac{dc_i}{dx} \tag{22}$$

where N_i is the flux rate of species i (kmol m^{-2} s^{-1}).

At steady-state conditions the equations of total sulphur content and total charge, involved in the desorption process are:

Total sulphur:

$$D_{H_2S} \frac{d^2[H_2S]}{dx^2} + D_{HS^-} \frac{d^2[HS^-]}{dx^2} = 0 \tag{23}$$

Charge:

$$D_{H^+} \frac{d^2[H^+]}{dx^2} - D_{HS^-} \frac{d^2[HS^-]}{dx^2} - D_{OH^-} \frac{d^2[OH^-]}{dx^2} = 0 \tag{24}$$

The reaction given by Eq. (15) and the autoprotolysis of water are instantaneous reactions.

The dissociation of H_2S:

$$K_1 = \frac{a_{H^+} a_{HS^-}}{a_{H_2S}} \tag{25}$$

The autoprotolysis of H_2O:

$$K_W = a_{H^+} a_{OH^-} \tag{26}$$

where K_1 is the equilibrium constant of the reaction given by Eq. (15), K_W represents autoprotolysis constant of water, a_i denotes activity of species i.

To solve the equation given above, proper boundary conditions must be defined. The boundary conditions at the interface ($x = \delta$) between liquid bulk and liquid film side are the bulk concentrations of the different species. For the interface at $x = 0$, Eqs. (25) and (26) are applicable together with:

$$-D_{H_2S} \frac{d[H_2S]}{dx} - D_{HS^-} \frac{d[HS^-]}{dx} = k_G(P^0_{H_2S} - P'_{H_2S}) \tag{27}$$

$$-D_{H^+} \frac{d[H^+]}{dx} = -D_{HS^-} \frac{d[HS^-]}{dx} - D_{OH^-} \frac{d[OH^-]}{dx} \tag{28}$$

where D_i represents the diffusivity of species i (m^2 s^{-1}), k_G denotes the gas phase mass transfer coefficient for H_2S (kmol Pa^{-1} m^{-2} s^{-1}), $P^0_{H_2S}$ represents partial pressure of H_2S in gas bulk (Pa), P'_{H_2S} denotes partial pressure of H_2S at the interface (Pa).

Eq. (27) states that the flux rate of total sulphur throughout the liquid film is equal to the flux rate of H_2S throughout the gas film. Eq. (28) shows simply that the net flux rate of the charged species is zero. The values, calculated with both models, are shown in comparison to the experimentally

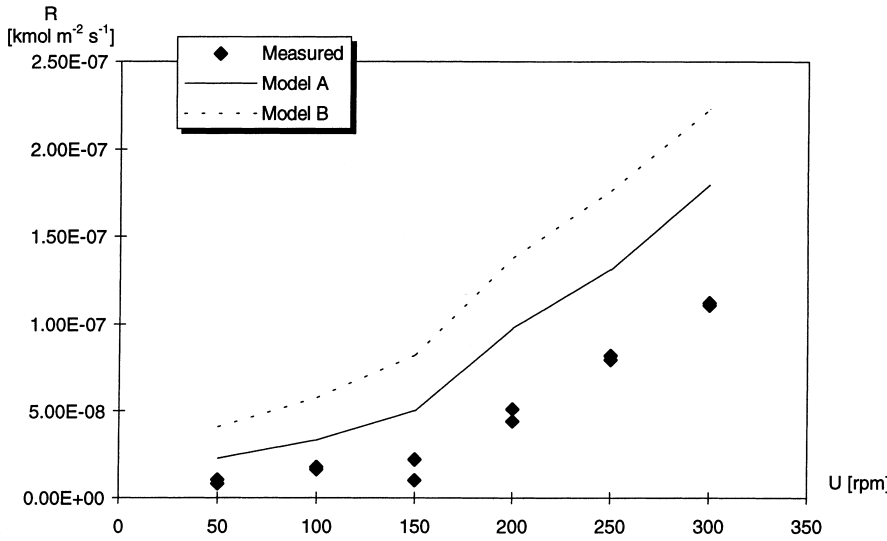

Fig. 6. Comparison between calculated and measured values for the desorption rate of H_2S from a 0.075 M Na_2S solution at pH 9 and 20°C.

detected values, see Figs. 6 and 7. Model A is based on physical desorption of aqueous H_2S. Model B includes chemical reactions with HS^- ions in the liquid film together with transport processes. Model B also predicts an enhancement effect from the Eq. (15). However, there is no support from the experimental data for such an enhancement effect. At pH 10 the desorption rate is well described by Model A and at pH 9 both models yield a too high prediction of the desorption rate. To conclude, Model A yields the best correlation to the experimental values at both pH values investigated.

5.2. Desorption model for CO_2

At high pH values (pH > 8), CO_2 reacts according to the reaction path with a finite reaction rate:

$$CO_2 + OH^- \leftrightarrow HCO_3^- \tag{29}$$

The HCO_3^- from Eq. (29) may be dissociated further via the instantaneous reaction:

$$HCO_3^- \leftrightarrow H^+ + CO_3^{2-} \tag{30}$$

At steady state the bulk reaction rate of CO_2 is equal to the desorption rate of CO_2 and the material balance has the form:

$$\frac{V}{a} r_{CO_2} = R_{CO_2} \tag{31}$$

where r_{CO_2} is the reaction rate of the chemical reaction forming CO_2 (kmol m^{-3} s^{-1}), R_{CO_2} represents desorption rate of CO_2 (kmol m^{-3} s^{-1}), V is the volume of the liquid phase (m^3), a represents the interfacial area (m^2).

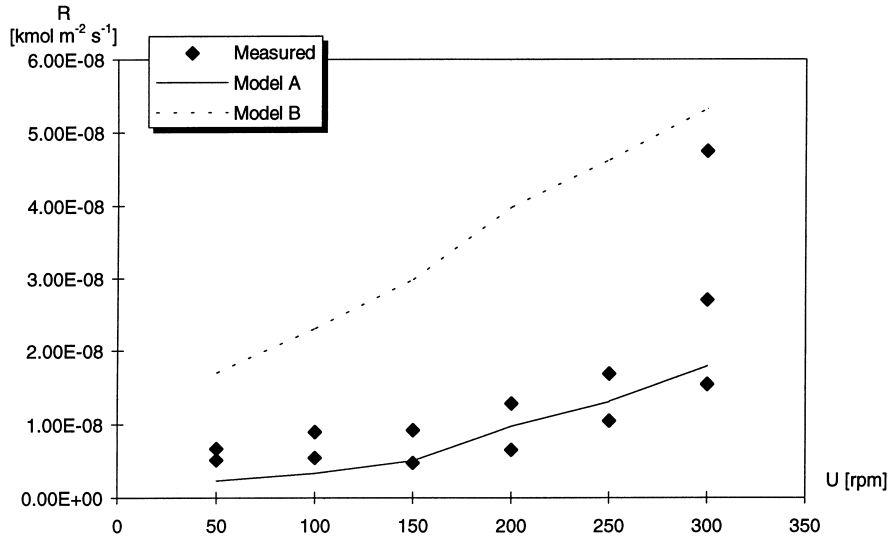

Fig. 7. Comparison between calculated and measured values for the desorption rate of H_2S from a 0.075 M Na_2S solution at pH 10 and 20°C.

The expressions for r_{CO_2} and R_{CO_2} are:

$$r_{CO_2} = \left(-k_{OH}[CO_2][OH^-] + k'_{OH}[HCO_3^-]\right) \quad (32)$$

$$R_{CO_2} = K_L\left([CO_2] - [CO_2]^0\right) \quad (33)$$

where k_{OH} is the reaction rate constant of Eq. (29) ($m^3\,kmol^{-1}\,s^{-1}$), k'_{OH} is the reaction rate of constant of the reverse reaction Eq. (29) (s^{-1}), K_L is the total mass transfer coefficient for the liquid side ($m\,s^{-1}$).

The concentration of CO_2 in the gas bulk is assumed to be zero due to the small amount of desorbed CO_2 and the continuous purge gas flow of nitrogen. This assumption modifies Eq. (33) to the following equation:

$$R_{CO_2} = K_L[CO_2] \quad (34)$$

Eqs. (32) and (34) are inserted into Eq. (31). Rearrangement gives the concentration of CO_2 in the liquid bulk phase:

$$[CO_2] = \frac{Vk'_{OH}[HCO_3^-]}{(K_L a + Vk_{OH}[OH^-])} \quad (35)$$

The total mass transfer coefficient for the liquid side can be calculated by:

$$\frac{1}{K_L} = \frac{1}{k_G He} + \frac{1}{k_L E} \quad (36)$$

where k_G is the gas side mass transfer coefficient for CO_2 ($kmol\,Pa^{-1}\,m^{-2}\,s^{-1}$), He represents Henry coefficient for CO_2 ($Pa\,m^3\,kmol^{-1}$), k_L is the liquid side mass transfer coefficient for CO_2 ($m\,s^{-1}$).

Eq. (34) has been evaluated under the assumption that the enhancement factor E of the desorption process is equal to 1. Control calculations showed values for E, which are close to 1. This confirms the above assumption, and the desorption process is not enhanced by a chemical reaction. A maximum value of E can be estimated using the film theory considering only the backward reaction of Eq. (29) and with a $[HCO_3^-]$ value as high as possible throughout the film, that is its bulk value.

Another aspect that can be considered is which step is rate controlling. By focusing the interest on Eq. (35) it can be distinguished between two cases:

Case 1:

$$Vk_{OH}[OH^-] \gg K_L a \quad (37)$$

Case 2:

$$Vk_{OH}[OH^-] \ll K_L a \quad (38)$$

Case 1 indicates that the concentration of CO_2 is constant and the process is transport controlled. The desorption rate is expressed by:

$$R = K_L[CO_2]_{eq} \quad (39)$$

And Eq. (35) simplifies in this case to:

$$[CO_2]_{eq} = [CO_2] = \frac{k_{OH}[HCO_3^-]}{k'_{OH}[OH^-]} = \frac{[HCO_3^-]}{K_2[OH^-]} \quad (40)$$

Case 2 indicates that the process is reaction controlled. Eq. (35) simplifies in this case to:

$$[CO_2] = \frac{Vk'_{OH}[HCO_3^-]}{K_L a} \quad (41)$$

With Eq. (34) the desorption rate is calculated by:

$$R = \frac{Vk'_{OH}}{a}[HCO_3^-] \quad (42)$$

In the present system, the desorption rate of CO_2 from a $NaHCO_3$ solution with the concentration of 0.2 $kmol\,m^{-3}$ at pH 9 and 10 at 20°C is transport controlled. After calculating E and finding that E is approximately 1, Eqs. (39) and (40) have been employed to calculate the theoretical values of the desorption rate. The values are calculated for the case of CO_2 desorption from a $NaHCO_3$ solution with the concentration of 0.2 $kmol\,m^{-3}$, see Figs. 8 and 9. The figures show that the experimental desorption rates of CO_2 are well described by the suggested desorption model.

5.3. Coefficients and factors used for the calculations with the models

The values for the coefficients and factors used in the models are calculated by Eqs. (43)–(50) which were obtained from Ref. [7]. Diffusion constants in water at 25°C are shown in Table 6. They are for infinite dilution, but at least in real systems any potential gradient will be dispersed by the high ionic content of the liquid phase. Diffusivities at other temperatures than at 25°C are obtained by:

$$D_T = D_{25}1.69T e^{-1854/T} \quad (43)$$

where D_T is the diffusivity of species i at temperature T ($m^2\,s^{-1}$), D_{25} is the diffusivity of species i at 25°C ($m^2\,s^{-1}$), T represents the temperature (K).

The equations for the calculation of the different constants are given below:

$$\log_{10}He_{CO_2} = -103.3809 - 0.01985076T + \frac{6919.53}{T} + 40.45154\log_{10}T - \frac{669365}{T^2} \quad (44)$$

$$\log_{10}He_{H_2S} = 2.7896 + 0.031459T - 4.81046 \times 10^{-5}T^2 - \frac{672.791}{T} + 0.144237\log_{10}T \quad (45)$$

Table 6
Diffusivities in H_2O at 25°C

Diffusivities ($m^2\,s^{-1}$)	25°C
H^+	9.31×10^{-9}
H_2S	1.41×10^{-9}
HS^-	1.74×10^{-9}
CO_2	2.00×10^{-9}
HCO_3^-	1.18×10^{-9}
CO_3^{2-}	0.96×10^{-9}
OH^-	5.24×10^{-9}

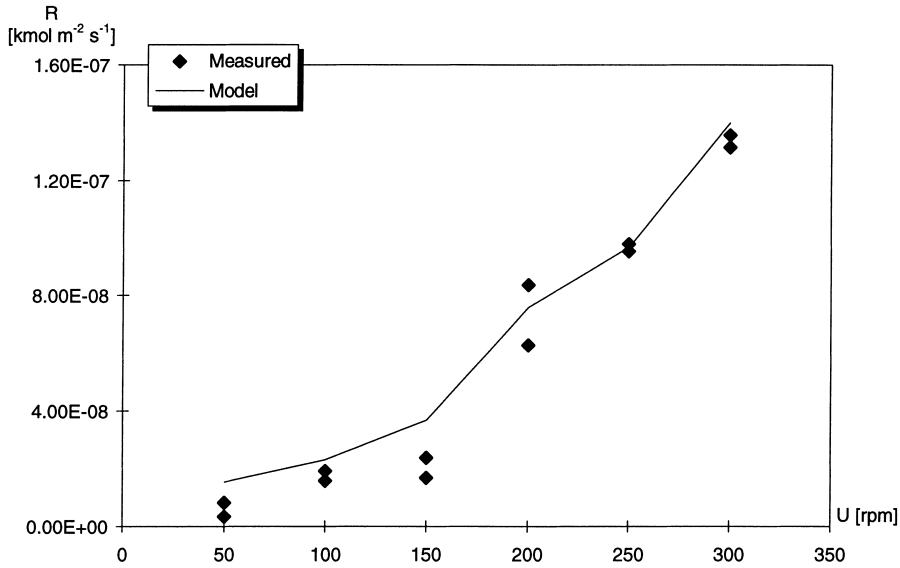

Fig. 8. Comparison between calculated and measured values for the desorption rate of CO_2 from a 0.2 M $NaHCO_3$ solution at pH 9 and 20°C.

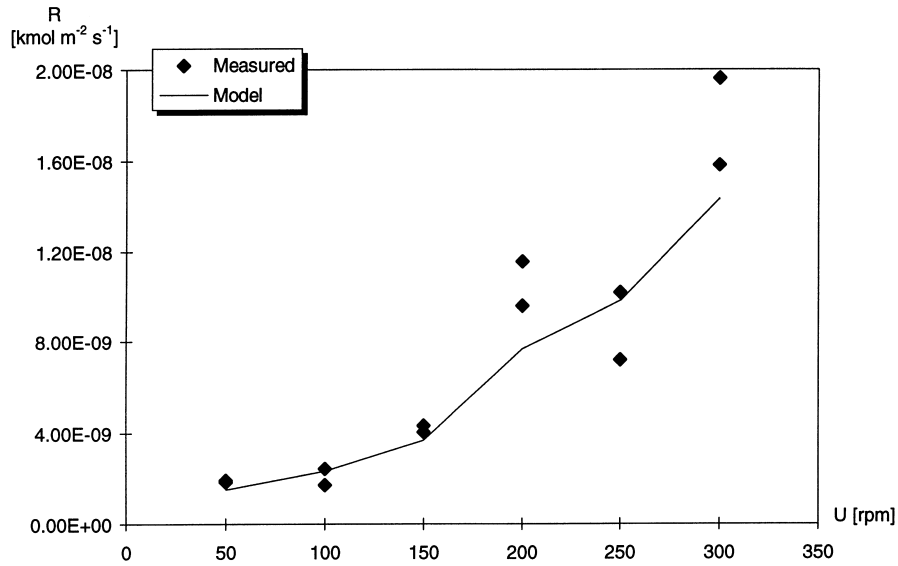

Fig. 9. Comparison between calculated and measured values for the desorption rate of CO_2 from a 0.2 M $NaHCO_3$ solution at pH 10 and 20°C.

$$\log_{10}K_1 = -\frac{3760}{T} - 20\log_{10}T + 55.06 \quad (46)$$

$$\log_{10}K_2 = -356.3094 - 0.06091964T + \frac{21834.37}{T} + 126.8339\log_{10}T - \frac{1684915}{T^2} \quad (47)$$

$$\log_{10}K_3 = -107.8871 - 0.03252849T + \frac{5151.79}{T} + 38.9256\log_{10}T - \frac{563713.9}{T^2} \quad (48)$$

$$\log_{10}K_W = -\frac{5839.50}{T} - 22.4773\log_{10}T + 61.2062 \quad (49)$$

$$\log_{10}k_{OH} = 13.635 - \frac{2895}{T} \quad (50)$$

where T is the temperature (K), He is the Henry coefficient (atm m^3 $kmol^{-1}$), K_1 is the 1st dissociation constant of H_2S, K_2 is the 1st dissociation constant of CO_2, K_3 is 2nd dissociation constant of CO_2, K_W represents autoprotolysis constant of water, k_{OH} is the reaction rate constant for Eq. (1) (m^3 $kmol^{-1}$ s^{-1}).

6. Simultaneous desorption of H_2S and CO_2 from synthetic green liquor

H_2S and CO_2 were desorbed simultaneously from a synthetic green liquor in the test facility described in Section 2. Experiments were performed at pH 9 and 10 with stirrer velocities in the range from 50 to 300 rpm. The

Table 7
Desorption rates of CO_2 at pH 9 and 10 from synthetic green liquor

U (rpm)	R ($kmol^{-2}\,s^{-1}$) pH 9	R ($kmol^{-2}\,s^{-1}$) pH 10
50	1.45×10^{-8}	9.68×10^{-10}
50	1.13×10^{-8}	4.78×10^{-10}
100	1.73×10^{-8}	2.04×10^{-9}
100	2.14×10^{-8}	2.54×10^{-9}
150	3.47×10^{-8}	1.05×10^{-9}
150	5.95×10^{-8}	1.55×10^{-9}
200	8.29×10^{-8}	3.90×10^{-9}
200	9.65×10^{-8}	5.09×10^{-9}
250	1.14×10^{-8}	4.99×10^{-9}
250	2.06×10^{-8}	6.38×10^{-9}
300	1.91×10^{-8}	4.98×10^{-9}
300	2.44×10^{-8}	7.73×10^{-9}

synthetic green liquor was a mixture of 0.055 kmol m^{-3} Na_2S solution and 0.2 kmol m^{-3} $NaHCO_3$ solution. These concentrations are of course not the same as in a real green liquor but they have the same concentration ratio [23]. Real green liquor was not used due to its high pH value, pH 12, and high concentrations of sulphide and carbonate compounds which are difficult to handle in a laboratory scale equipment. The results of the experiments are shown in Tables 7 and 8.

The amounts of desorbed gases are measured with a mass spectrometer [19]. The used analysis matrix consists of three compounds, H_2S, CO_2 and Ar. The calibration of the mass spectrometer for H_2S was performed with a gas mixture containing 1000 ppm H_2S, 48.9% Ar and 51% N_2. For the calibration of the mass spectrometer with respect to CO_2 a hand blended gas mixture with 500 ppm CO_2 was used. The source gas contained 13% CO_2 and 87% Ar and as dilution gas 100% N_2 was used. The calibration of the mass spectrometer was performed until two successive measurements showed almost the same calibration factors. Then the calibration session was ended and the reactor was prepared for running an experiment. The preparation of the reactor for an experiment included the filling with distilled water (approximate pH value was adjusted by HCl or NaOH solution), followed by the addition of the chemicals and adjustment of the pH value of the obtained synthetic green liquor. The fine adjustment of the pH value was also done by HCl or NaOH solution. The volume of added base or acid was negligible compared with the total volume.

Table 8
Desorption rates of H_2S at pH 9 and 10 from synthetic green liquor

U (rpm)	R ($kmol^{-2}\,s^{-1}$) pH 9	R ($kmol^{-2}\,s^{-1}$) pH 10
50	2.40×10^{-7}	2.52×10^{-8}
50	1.89×10^{-7}	2.58×10^{-8}
100	2.76×10^{-7}	3.04×10^{-8}
100	3.32×10^{-7}	3.32×10^{-8}
150	3.29×10^{-7}	3.02×10^{-8}
150	4.32×10^{-7}	3.09×10^{-8}
200	3.93×10^{-7}	3.40×10^{-8}
200	4.57×10^{-7}	4.09×10^{-8}
250	4.22×10^{-7}	3.45×10^{-8}
250	6.59×10^{-7}	3.71×10^{-8}
300	5.53×10^{-7}	3.44×10^{-8}
300	6.27×10^{-7}	4.24×10^{-8}

During the experiments the pH value was not held constant by the pH-stat. This was not necessary as the observed pH value was not changing very much during an experiment. Especially at pH 10 the pH value was very constant during an experiment, within a maximum pH error of 0.05 units from the adjusted pH value. For pH 9 the maximum error was 0.1 units from the adjusted pH value. Therefore, the pH-stat was only used for scanning the pH value during the experiments of simultaneous desorption of H_2S and CO_2 from synthetic green liquor. The error due to the changing pH value during an experiment is negligible as the pH value at the beginning of an experiment was adjusted to within 0.05 pH units of the desired pH value of pH 9 or 10.

7. Modelling the simultaneous desorption of H_2S and CO_2 from green liquor

7.1. Desorption model for H_2S

The model used, is basically the same as the Model B described in Section 5.1. Changes have been done as the species HCO_3^- present in the liquor must be considered as proton donator in the desorption process of H_2S from green liquor. Following chemical reaction equations describe the desorption process of H_2S:

$$HS^- + H^+ \leftrightarrow H_2S\,(aq) \tag{51}$$

$$HCO_3^- \leftrightarrow H^+ + CO_3^{2-} \tag{52}$$

The desorption model includes Eqs. (23), (25) and (26) together with an additional balance of total carbonate:

$$D_{CO_3^{2-}} \frac{d^2[CO_3^{2-}]}{dx^2} + D_{HCO_3^-} \frac{d^2[HCO_3^-]}{dx^2} = 0 \tag{53}$$

a modified charge balance:

$$D_{H^+} \frac{d^2[H^+]}{dx^2} - D_{HS^-} \frac{d^2[HS^-]}{dx^2} - D_{OH^-} \frac{d^2[OH^-]}{dx^2} - D_{HCO_3^-} \frac{d^2[HCO_3^-]}{dx^2} - 2D_{CO_3^{2-}} \frac{d^2[CO_3^{2-}]}{dx^2} = 0 \tag{54}$$

and the dissociation of HCO_3^-:

$$K_2 = \frac{a_{CO_3^{2-}} a_{H^+}}{a_{HCO_3^-}} \tag{55}$$

where K_2 is the equilibrium constant of the reaction given by Eq. (52), a_i is the activity of species i.

The boundary conditions at the interface ($x = \delta$) between liquid bulk and liquid film side are the bulk concentrations of the different species. For the interface at $x = 0$, Eqs. (25), (26) and (55) are applicable together with Eqs. (23), (56)

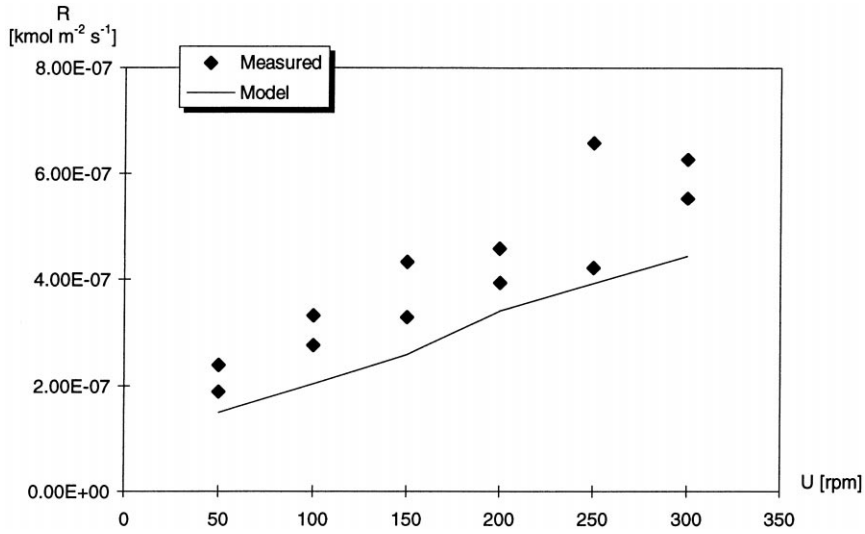

Fig. 10. Comparison between calculated and measured values for the desorption rate of H_2S from synthetic green liquor at pH 9 and 20°C.

and (57).

$$-D_{HCO_3^-}\frac{d[HCO_3^-]}{dx} - D_{CO_3^{2-}}\frac{d[CO_3^{2-}]}{dx} = 0 \quad (56)$$

and

$$-D_{H^+}\frac{d[H^+]}{dx} = -D_{HS^-}\frac{d[HS^-]}{dx} - D_{OH^-}\frac{d[OH^-]}{dx} - D_{HCO_3^-}\frac{d[HCO_3^-]}{dx} - 2D_{CO_3^{2-}}\frac{d[CO_3^{2-}]}{dx} \quad (57)$$

where D_i is the diffusivity of species i ($m^2 s^{-1}$), k_G is the gas phase mass transfer coefficient for H_2S (kmol $Pa^{-1}\,m^{-2}\,s^{-1}$), $P^0_{H_2S}$ is the partial pressure of H_2S (Pa), P'_{H_2S} represents the partial pressure of H_2S at the interface (Pa).

Theoretical and experimental values for the desorption of H_2S from liquor at pH 9 and 10 are shown in Figs. 10 and 11. In this system at both pH 9 and 10, a large enhancement effect from Eq. (51) is present, mainly through the buffering capacity of the carbonate system Eq. (52). This effect is predicted by the model and also indicated by the experimental data. The increase in H_2S desorption rates is significant when carbonates are present in the solution.

When considering diffusion of charged species, an electric potential gradient would normally arise due to different mobilities/diffusivities of the charged species involved. A potential gradient affects the flux rate of the transport process according to the Nernst–Planck equation [24]. The analysis with a potential gradient complicates the model considerably and has been neglected in the present work.

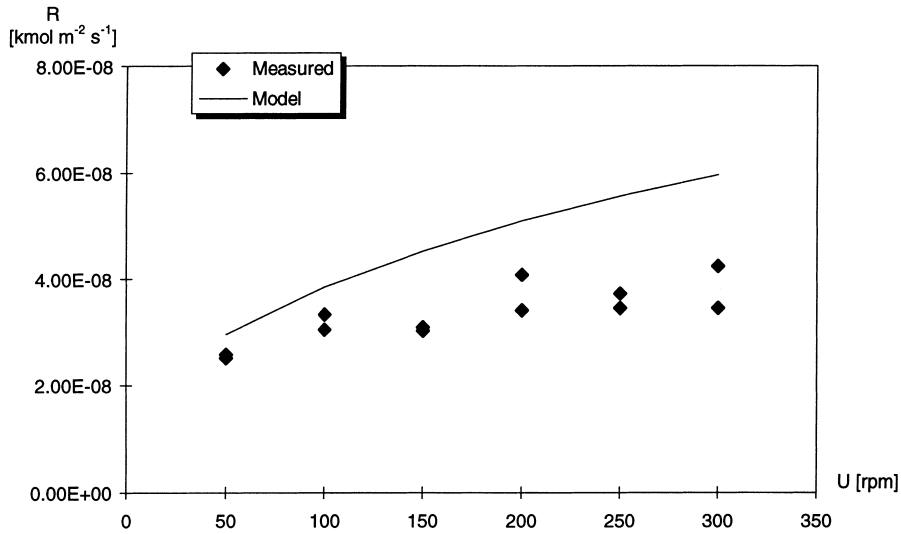

Fig. 11. Comparison between calculated and measured values for the desorption rate of H_2S from synthetic green liquor at pH 10 and 20°C.

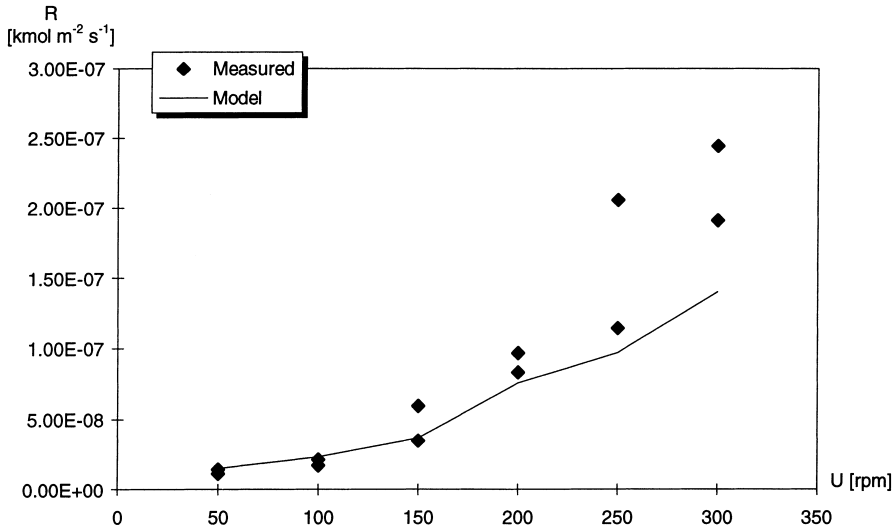

Fig. 12. Comparison between calculated and measured values for the desorption rate of CO_2 from synthetic green liquor at pH 9 and 20°C.

In a real green liquor system we have high salts concentration of species not directly involved in desorption reactions. The motion of these charged species, the ionic buffer, would effectively disperse any electric potential gradient formed.

Considering the ionic strength effect on equilibria, good correlations are available to predict activity coefficients even at high ionic strengths. Commercial softwares for complex thermodynamic calculations are also available, for example the OLI system [25]. In green liquor no pulp is present.

To conclude, the desorption model should be applicable in real green liquor system, however, appropriate activity coefficients must be used.

7.2. Desorption model of CO_2

The experimental values for the desorption of CO_2 from green liquor are in good agreement with the theoretical values calculated with the model, described in Section 5.2. Therefore, no new model was introduced and the theoretical values seen in Figs. 12 and 13 are the same as for individual desorption of CO_2 from $NaHCO_3$ solution.

7.3. Selectivity for H_2S

A key parameter in real systems is the selectivity of H_2S. This parameter judges if a separation process is meaningful or not and how far a process is flexible and economic. In the

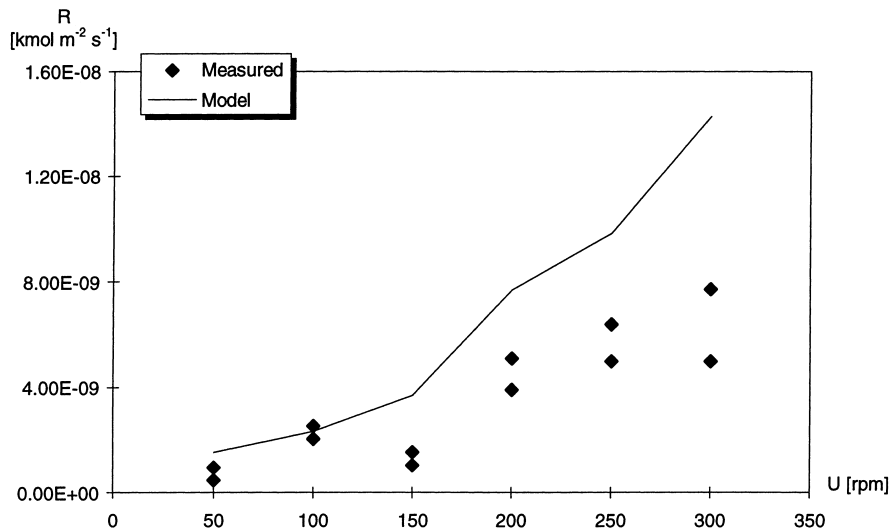

Fig. 13. Comparison between calculated and measured values for the desorption rate of CO_2 from synthetic green liquor at pH 10 and 20°C.

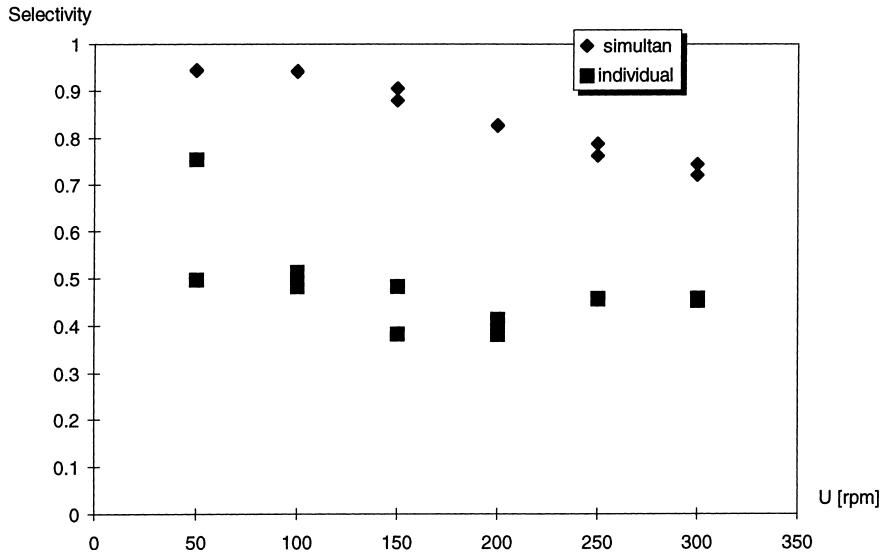

Fig. 14. Selectivity of the desorption process at pH 9.

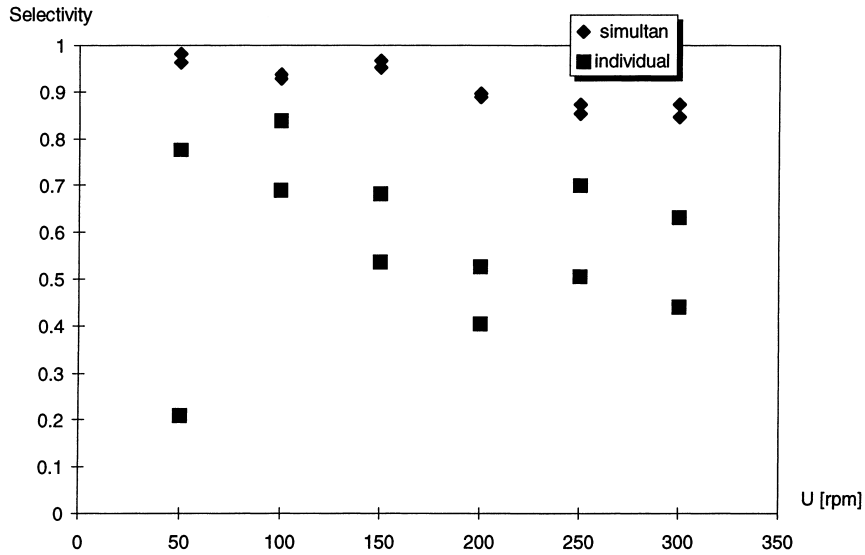

Fig. 15. Selectivity of the desorption process at pH 10.

present work the selectivity of the desorption process for H_2S is defined by:

$$S = \frac{R_{H_2S}}{R_{H_2S} + R_{CO_2}} \quad (58)$$

where S is the selectivity of H_2S, R_{H_2S} represents desorption rate of H_2S (kmol m^{-2} s^{-1}), R_{CO_2} is the desorption rate of CO_2 (kmol m^{-2} s^{-1}).

Figs. 14 and 15 show the calculated selectivity for simulations and individual desorption at pH 9 and 10. The simultaneous selectivity values are obtained from desorption experiments in synthetic green liquor. For the individual selectivity values a concept is used that assumes the individual desorption rates of H_2S and CO_2 in one system but not interacting with each other. From Figs. 14 and 15 it is clearly seen that the presence and interaction from carbonate ions has a positive effect on the selectivity for H_2S. The selectivity is improved by this effect, especially at pH 10 the selectivity is relatively high (>0.84) over the entire experimental range. At both pH values investigation of the selectivity for H_2S is increasing with decreasing impeller speeds due to lower mass transfer rates or thicker liquid films.

It is important to notice that the concentration of Na_2S between the simultaneous and individual desorption processes, plotted in Figs. 14 and 15 are slightly different. For the simultaneous desorption experiments the Na_2S concentration is 0.055 M and for the individual desorption the Na_2S

concentration is 0.075 M. The concentration of $NaHCO_3$ in all experiments is the same. The difference in Na_2S concentration between the simultaneous and individual desorption experiments, however, does not affect the shown trends in selectivity. On contrary, the difference between the selectivity for both processes should be even larger due to the higher driving force for H_2S in the individual H_2S desorption experiments.

8. Conclusions

The stripping of H_2S and CO_2 from a synthetic green liquor has been researched. The gases were first studied individually followed by simultaneous desorption. The synthetic green liquor was a mixture of 0.055 kmol m^{-3} Na_2S and 0.2 kmol m^{-3} $NaHCO_3$ solution, yielding the same concentration ratio as in real green liquor. The pH value was adjusted at 9 and 10 as the driving force for desorption must be sufficiently high and the composition not too far away from a real green liquor. The following conclusions are for simultaneous desorption of H_2S and CO_2 within the pH-interval investigated.

1. The CO_2 desorption is not enhanced by any chemical reaction and can be treated as an physical non-reacting system withdrawn from its chemical environment.
2. The H_2S desorption is enhanced by the presence of the buffering carbonate system. When desorbed without carbonates present no enhancement effect is obvious.
3. The selectivity for desorption of H_2S is improved when the carbonate system is present compared with a chemically uncoupled system.
4. The desorption system, at least in an ideal solution, can be described with a desorption model based on the film theory where diffusion is coupled with chemical reactions in a stagnant liquid film followed by transport throughout a gas film.
5. The selectivity increases with decreasing impeller speeds, that is lower mass transfer rates or thicker films.

Acknowledgements

The research work was economically supported by the Sodahuskommittén research programme Sulfatåtervinning/ Svartlutförgasning.

References

[1] L.L. Stigsson, Conf. TAPPI Pulping, San Diego, 1994.
[2] P. McKeough, VTT Publications 174, Espoo, 1994.
[3] P.V. Danckwerts, Gas–Liquid Reaction, McGraw-Hill, London, 1970.
[4] Y.T. Shah, M.M. Sharma, Trans. Inst. Chem. Eng. 54 (1976) 1–41.
[5] S.M. Yih, C.C. Sun, Chem. Eng. J. 34 (1987) 65–72.
[6] S.M. Yih, H.C. Lai, Chem. Eng. Commun. 51 (1987) 277–290.
[7] M. Wallin, S. Olausson, Chem. Eng. Commun. 123 (1993) 43–59.
[8] L.A. Arrua, B.J. McCoy, J.M. Smith, AlChE J. 36 (1990) 1768–1772.
[9] W.T. Koetsier, D. Thoenes, Chem. Eng. J. 5 (1973) 71–75.
[10] N.C. Panja, D.P. Rao, Chem. Eng. J. 52 (1993) 121–129.
[11] K.A. Ramanarayanan, M.M. Sharma, Ind. Eng. Chem. Process Des. Dev. 21 (1982) 353–355.
[12] R.S. Albal, Y.T. Shah, A. Schumpe, Chem. Eng. J. 27 (1938) 61–80.
[13] I.T. Hassan, C.W. Robinson, AlChE J. 23 (1977) 48–56.
[14] V.D. Mehta, M.M. Sharma, Chem. Eng. Sci. 26 (1971) 461–479.
[15] S. Sideman, O. Hortacsu, J.W. Fulton, Ind. Eng. Chem. 58 (1966) 32–47.
[16] M. Teramoto, M. Ikeda, H. Teranishi, Int. Chem. Eng. 17 (1977) 265–270.
[17] K.R. Westerterp, L.L. van Dierendonck, J.A. de Kraa, Chem. Eng. Sci. 18 (1963) 157–176.
[18] M. Al-Wohoush, Thesis for the Degree of Master of Engineering, Department of Chemical Engineering, MCGill University, Montreal, Canada, 1994.
[19] Balzers Quadstar Plus/V3.0, User's Guide.
[20] V. Linek, T. Moucha, J. Sinkule. Chem. Eng. Sci. 51 (1996) 3203–3212.
[21] H.H. Topiwala, G. Hamer, Biotechnol. Bioeng. Symp. 4 (1973) 547–557.
[22] K. Onda, H. Takeuchi, T. Kobayashi, K. Yokata, J. Chem. Eng. Jpn 5 (1972) 27–33.
[23] L. Andersson, Personal Communication, Kvaerner Pulping.
[24] E.L. Cussler, Diffussion: Mass transfer in fluid systems, Cambridge University Press, New York, 1984.
[25] OLI Manual, OLI Software Inc., Morris Plains, New York, 1996.